

Numerical demonstration of the reciprocity among elemental relaxation and driven-flow problems for a rarefied gas in a channel

Shigeru Takata and Masashi Oishi

Citation: *Phys. Fluids* **24**, 012003 (2012); doi: 10.1063/1.3678308

View online: <http://dx.doi.org/10.1063/1.3678308>

View Table of Contents: <http://pof.aip.org/resource/1/PHFLE6/v24/i1>

Published by the [American Institute of Physics](#).

Related Articles

Response to “Comment on ‘Velocity slip coefficients based on the hard-sphere Boltzmann equation’” [*Phys. Fluids* **24**, 079101 (2012)]

[Phys. Fluids](#) **24**, 079102 (2012)

Investigation on heat transfer between two coaxial cylinders for measurement of thermal accommodation coefficient

[Phys. Fluids](#) **24**, 062002 (2012)

Preface to Special Topic: A Tribute to Carlo Cercignani (1939–2010)

[Phys. Fluids](#) **23**, 030501 (2011)

Boundary conditions at the vapor-liquid interface

[Phys. Fluids](#) **23**, 030609 (2011)

Sonine approximation for collisional moments of granular gases of inelastic rough spheres

[Phys. Fluids](#) **23**, 030604 (2011)

Additional information on Phys. Fluids

Journal Homepage: <http://pof.aip.org/>

Journal Information: http://pof.aip.org/about/about_the_journal

Top downloads: http://pof.aip.org/features/most_downloaded

Information for Authors: <http://pof.aip.org/authors>

ADVERTISEMENT



**Running in Circles Looking
for the Best Science Job?**

Search hundreds of exciting
new jobs each month!

<http://careers.physicstoday.org/jobs>

physicstodayJOBS



Numerical demonstration of the reciprocity among elemental relaxation and driven-flow problems for a rarefied gas in a channel

Shigeru Takata^{a)} and Masashi Oishi

*Department of Mechanical Engineering and Science, Kyoto University,
Kyoto 606-8501, Japan*

(Received 8 November 2011; accepted 3 January 2012; published online 26 January 2012;
corrected 2 February 2012)

Relaxations from a uniform mass/heat flow and flows driven by an external force/temperature-gradient for a rarefied gas between two parallel plates are studied on the basis of the kinetic theory of gases. By numerical computations of the linearized Bhatnagar–Gross–Krook model of the Boltzmann equation, it is demonstrated that the reciprocity among these elemental flows derived from a general reciprocity theory for time-dependent problems [S. Takata, *J. Stat. Phys.* **140**, 985 (2010)] holds at any time and any Knudsen numbers. Moreover, a propagation of the discontinuity of the velocity distribution function (VDF) in the relaxation problems and that of the derivative discontinuity of the VDF in the driven-flow problems are demonstrated. Their relation is also clarified. © 2012 American Institute of Physics. [doi:10.1063/1.3678308]

I. INTRODUCTION

Cross relation between different phenomena described by the linearized Boltzmann equation has been discussed or pointed out by various researchers from 1970s.^{1–7} They considered steady (or quasi-steady) systems and discussed a symmetry of thermodynamic fluxes when they express the entropy production as a sum of the products of the thermodynamic forces and conjugated thermodynamic fluxes. As pointed out in Refs. 2, 5, and 6 in the studies of slip coefficients and thermal polarization, however, Onsager's symmetry does not necessarily hold in its original spirit. The symmetry argument could be direct, transparent, and flexible, if we reconsider it from another viewpoint.

In fact, we have recently developed a general framework of the symmetry from a viewpoint of the Green function, which applies not only to steady systems^{8,9} but also to time-dependent systems,¹⁰ the latter of which contains some results similar to the linear response theory^{11,12} for systems of arbitrary Knudsen number. In the present paper, we provide a simple numerical demonstration of the symmetry for time-dependent problems which has been rarely discussed in the literature. More precisely, we consider a rarefied gas in a channel and study two relaxation problems from a uniform mass/heat flow and two driven-flow problems (flows caused by a uniform gravity/temperature-gradient). We numerically demonstrate the identities of fluxes among the four different problems on the basis of the Bhatnagar–Gross–Krook (BGK)^{13,14} model of the Boltzmann equation under the diffuse reflection condition. In the relaxation problems, as expected by a general discussion found in Refs. 15–17, the velocity distribution function (VDF) of gas molecules is discontinuous not only on the channel walls but also inside the gas. We call attentions of the reader to it, and moreover, point out that the derivative of VDF, not the VDF itself, is discontinuous in the driven-flow problems. This feature is explained in the connection to the discontinuity in the relaxation problems.

The paper is organized as follows. We first formulate elemental four problems, i.e., two driven-flow and two relaxation problems, in Sec. II and present the reciprocal relations of fluxes that hold among them in Sec. III. Then, in Sec. IV, we provide numerical results, which support

^{a)}Electronic mail: takata.shigeru.4a@kyoto-u.ac.jp.

the reciprocity presented in Sec. III and illustrate the propagation of discontinuities of the VDF and its derivative in the relaxation and driven-flow problems, respectively.

II. PROBLEM

Consider a rarefied gas between two parallel plates separated by a distance D . We denote a position vector by $D\mathbf{x}$ and introduce the rectangular coordinates such that the two plates are located at $x_1 = \pm 1/2$. Hence, the x_1 -direction is normal to the plates, while the x_2 - and x_3 -directions are parallel to the plates. We assume that (i) the gas behavior is described by the Bhatnagar–Gross–Krook (BGK) model^{13,14} kinetic equation and that (ii) the gas molecules are diffusely reflected on the plates. We investigate the gas behavior in the following four cases where the deviation from the reference resting equilibrium state with density ρ_0 and temperature T_0 is so small that the linearization of the equation and boundary condition is allowed. In what follows, the time is denoted by $t_0 t$, the molecular velocity by $(2RT_0)^{1/2} \boldsymbol{\zeta}$, the velocity distribution function by $\rho_0 (2RT_0)^{-3/2} (1 + \psi) E$ with $E = \pi^{-3/2} \exp(-|\boldsymbol{\zeta}|^2)$, where R is the specific gas constant and $t_0 = D/(2RT_0)^{1/2}$ is a reference time. The four cases are

(DP) The plates are maintained at the reference temperature T_0 . Initially, the gas is in the reference resting equilibrium state, i.e., $\psi = 0$ at $t = 0$, and a uniform external force $(0, -F, 0)$ per molecule is acting on the gas. Here the ratio $C_{DP} = FD/mRT_0$ (m is the mass of a molecule) is small, i.e., $|C_{DP}| \ll 1$.

(DT) The plates are maintained at temperature $T_0(1 + C_{DT}x_2)$ ($|C_{DT}| \ll 1$). Initially, the gas is at rest with the reference pressure $p_0 = \rho_0 RT_0$ and the same temperature distribution as the plates,¹⁸ i.e., $\psi = C_{DT}x_2(|\boldsymbol{\zeta}|^2 - 5/2)$ at $t = 0$.

(RP) The plates are maintained at the reference temperature T_0 . Initially, the gas flows uniformly with the velocity $(0, -U, 0)$, i.e., $\psi = -2[U/(2RT_0)^{1/2}] \zeta_2$ at $t = 0$. Here, $C_{RP} = 2U/(2RT_0)^{1/2}$ is small ($|C_{RP}| \ll 1$).

(RT) The plates are maintained at the reference temperature T_0 . Initially, there is a uniform heat flow $(0, -q, 0)$ in the gas,¹⁸ i.e., $\psi = -2[q/p_0(2RT_0)^{1/2}] \zeta_2 (|\boldsymbol{\zeta}|^2 - 5/2)$ at $t = 0$. Here, $C_{RT} = 2q/p_0(2RT_0)^{1/2}$ is small ($|C_{RT}| \ll 1$).

See Fig. 1 for the schematic of each case. Hereinafter, we put the subscript index $\alpha = DP, DT, RP, RT$ to the quantities, e.g., ψ_{DP} , in order to identify the problem.

In the above four cases, we can seek the solution ψ_α in the form

$$\begin{aligned}\psi_{DP}(t, \mathbf{x}, \boldsymbol{\zeta}) &= C_{DP} \phi_{DP}(t, x_1, \boldsymbol{\zeta}), \\ \psi_{DT}(t, \mathbf{x}, \boldsymbol{\zeta}) &= C_{DT} \left[x_2 \left(|\boldsymbol{\zeta}|^2 - \frac{5}{2} \right) + \phi_{DT}(t, x_1, \boldsymbol{\zeta}) \right], \\ \psi_{RP}(t, \mathbf{x}, \boldsymbol{\zeta}) &= C_{RP} \phi_{RP}(t, x_1, \boldsymbol{\zeta}), \\ \psi_{RT}(t, \mathbf{x}, \boldsymbol{\zeta}) &= C_{RT} \phi_{RT}(t, x_1, \boldsymbol{\zeta}),\end{aligned}$$

where $\phi_\alpha(t, x_1, \boldsymbol{\zeta})$ is a function such that $\phi_\alpha(-\zeta_2) = -\phi_\alpha(\zeta_2)$ and $\phi_\alpha(-\zeta_3) = \phi_\alpha(\zeta_3)$, and the problem is reduced to the following initial- and boundary-value problem for ϕ_α :

$$\frac{\partial \phi_\alpha}{\partial t} + \zeta_1 \frac{\partial \phi_\alpha}{\partial x_1} = \frac{1}{k} (-\phi_\alpha + 2(\zeta_2 \phi_\alpha) \zeta_2) + I_\alpha, \quad (1a)$$

$$\phi_\alpha = 0, \quad \left(\zeta_1 \leq 0, \quad x_1 = \pm \frac{1}{2} \right), \quad (1b)$$

$$\phi_\alpha = \phi_\alpha^{\text{in}}, \quad (t = 0), \quad (1c)$$

where

$$I_{DP} = -\zeta_2, \quad \phi_{DP}^{\text{in}} = 0, \quad (1d)$$

$$I_{DT} = -\zeta_2 \left(|\boldsymbol{\zeta}|^2 - \frac{5}{2} \right), \quad \phi_{DT}^{\text{in}} = 0, \quad (1e)$$

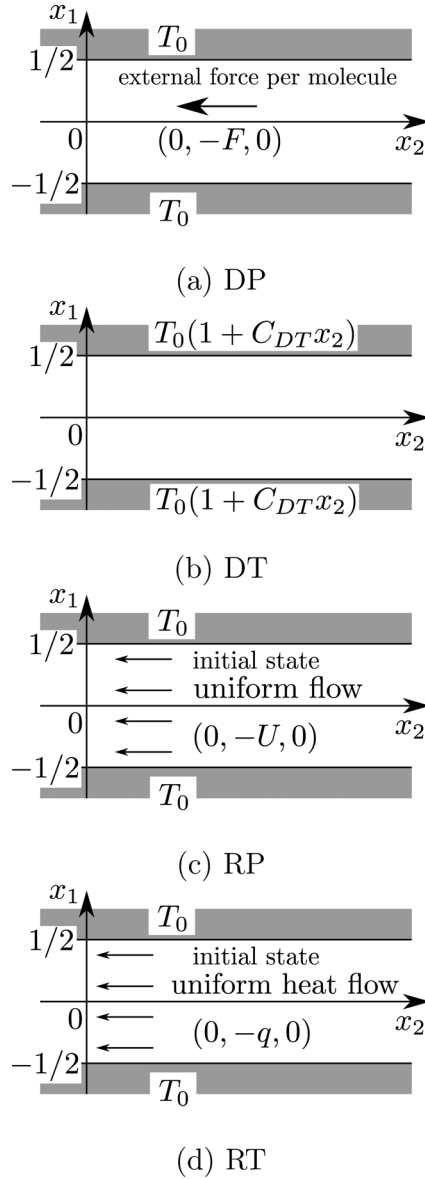


FIG. 1. Schematic of the problems.

$$I_{RP} = 0, \quad \phi_{RP}^{in} = -\zeta_2, \quad (1f)$$

$$I_{RT} = 0, \quad \phi_{RT}^{in} = -\zeta_2 \left(|\zeta|^2 - \frac{5}{2} \right). \quad (1g)$$

Here

$$\langle f \rangle = \int f(\zeta) E(\zeta) d\zeta, \quad k = \frac{\sqrt{\pi} \ell_0}{2D},$$

and ℓ_0 is the mean free path of a gas molecule at the reference equilibrium state, i.e., $\ell_0 = (2/\sqrt{\pi})(2RT_0)^{1/2}/(A\rho_0)$, where A is a constant such that $A\rho_0$ is a collision frequency. In Eq. (1a), the moments $\langle \phi_\alpha \rangle$ and $\langle |\zeta|^2 \phi_\alpha \rangle$ have already vanished because ϕ_α is odd with respect to ζ_2 .

The flow velocity $(2RT_0)^{1/2}C_\alpha(0, u_\alpha, 0)$, heat flow vector $p_0(2RT_0)^{1/2}C_\alpha(0, Q_\alpha, 0)$, and the mass and heat flow rates $\rho_0(2RT_0)^{1/2}DC_\alpha M_\alpha$ and $p_0(2RT_0)^{1/2}DC_\alpha H_\alpha$ per unit length in Dx_3 are given by

$$u_\alpha = \langle \zeta_2 \phi_\alpha \rangle, \quad M_\alpha = \int_{-1/2}^{1/2} u_\alpha dx_1,$$

$$Q_\alpha = \left\langle \zeta_2 \left(|\zeta|^2 - \frac{5}{2} \right) \phi_\alpha \right\rangle, \quad H_\alpha = \int_{-1/2}^{1/2} Q_\alpha dx_1.$$

III. RECIPROCITY OF FLUXES

Applying a symmetric relation for time-dependent problems developed in Ref. 10 to the present four problems, we find that the identity

$$\int_{-1/2}^{1/2} \langle \phi_\beta^{in} \phi_\alpha \rangle dx_1 + \int_{-1/2}^{1/2} \int_0^t \langle I_\beta \phi_\alpha \rangle dt dx_1 = \int_{-1/2}^{1/2} \langle \phi_\alpha^{in} \phi_\beta \rangle dx_1 + \int_{-1/2}^{1/2} \int_0^t \langle I_\alpha \phi_\beta \rangle dt dx_1, \quad (2)$$

holds for any pair of $\{\alpha, \beta\} = \{DP, DT, RP, RT\}$, where we have used the parity of I_α and ϕ_α and the fact that I_α is independent of t . The non-trivial six identities, i.e., Eq. (2) for $\alpha \neq \beta$, can be reduced to three equations:

$$\int_0^t M_{RT} dt = H_{DP} = M_{DT} = \int_0^t H_{RP} dt, \quad (3a)$$

$$M_{DP} = \int_0^t M_{RP} dt, \quad (3b)$$

$$H_{DT} = \int_0^t H_{RT} dt. \quad (3c)$$

Here, the second equality in Eq. (3a) is obtained by taking a time derivative of the identity (2) for $\{\alpha, \beta\} = \{DP, DT\}$. The identity (2) for $\{\alpha, \beta\} = \{RP, RT\}$ is omitted here because it is obtained by taking a time derivative of Eq. (3a). It should be noted that the above identities hold for any time and any Knudsen number. The physical meanings of the identities are as follows:

1. Heat flow rate H_{DP} driven by the external force is identical to the mass flow rate M_{DT} driven by the temperature gradient. Moreover, they are identical to the time integration of the mass flow rate $\int_0^t H_{RP} dt$ in the relaxation from the uniform heat flow and that of the heat flow rate $\int_0^t M_{RT} dt$ in the relaxation from the uniform flow.
2. Mass flow rate M_{DP} driven by the external force is identical to the time integration of the mass flow rate $\int_0^t M_{RP} dt$ in the relaxation from the uniform flow.
3. Heat flow rate H_{DT} driven by the temperature gradient is identical to the time integration of the heat flow rate $\int_0^t H_{RT} dt$ in the relaxation from the uniform heat flow.

In the next section, the above identities are numerically demonstrated to hold.

IV. NUMERICAL RESULTS AND DISCUSSIONS

For actual numerical computations, we introduce marginal VDFs

$$F_\alpha(t, x_1, \zeta_1) = \sqrt{\pi} \int_{-\infty}^{\infty} \int_{-\infty}^{\infty} \phi_\alpha E d\zeta_2 d\zeta_3,$$

$$G_\alpha(t, x_1, \zeta_1) = \sqrt{\pi} \int_{-\infty}^{\infty} \int_{-\infty}^{\infty} \left(|\zeta|^2 - \frac{5}{2} \right) \phi_\alpha E d\zeta_2 d\zeta_3,$$

and transform the problem (1) into that for F_α and G_α (Chu's method). In order to obtain the flow velocity u_α , it is enough to solve the problem for F_α , which is closed. In order to obtain the heat

flow Q_x , however, it is necessary to solve the problem for G_x , which is not closed and is dependent of F_x through u_x .

As demonstrated later, the VDF and its derivative can be discontinuous not only on the plates but also in the gas.¹⁵ In order to handle it properly, we adopt a hybrid finite difference scheme which was first developed in Ref. 15 to avoid a finite difference across the discontinuity. It is a hybrid between a standard finite difference for t and x_1 and a finite difference along the characteristics on which the discontinuities propagate. The details of the method are described in Ref. 19 and thus are omitted here. Our scheme is basically upwind second-order in x_1 and first-order in t . The data presented below are obtained by the following computational condition: the time step 5×10^{-5} , a non-uniform grid for x_1 which is symmetric with respect to $x_1 = 0$ and divides the region $-1/2 \leq x_1 \leq 1/2$ into 200 intervals, and a nonuniform grid for ζ_1 which is symmetric with respect to $\zeta_1 = 0$ and divides the region into 116 intervals after restricting the region to $|\zeta_1| \leq 4.429$. The grid interval in x_1 is smallest ($\sim 5.0 \times 10^{-4}$) near the plates and is largest ($\sim 1.8 \times 10^{-2}$) around $x_1 = 0$. The grid interval in ζ_1 is smallest ($\sim 3.6 \times 10^{-3}$) around $\zeta_1 = 0$ and is largest ($\sim 2.2 \times 10^{-1}$) around $\zeta_1 = \pm 4.429$.

A. Flux reciprocity

Figure 2(a) shows the profiles of the heat flow Q_{DP} and the flow velocity u_{DT} at various time t in the case of $k = 1$, while Fig. 2(b) shows the profiles of the heat flow Q_{RP} and of the flow velocity u_{RT} . As clearly observed, the profiles are all different from one another. Nevertheless, Fig. 3 shows that the gross quantities H_{DP} , M_{DT} , $\int_0^t H_{RP} dt$, and $\int_0^t M_{RT} dt$ agree at any time t for any k , as the identity (3a) predicts. In the present computation, relative errors among these four quantities at sampling time $t = 0.01, 0.05, 0.10, 0.50, 1.00, 2.00, 3.00, 4.00, 8.00, 10.0, 15.0$ are bounded by 0.18%, 0.05%, and 0.02% for $k = 0.1, 1$, and 10, respectively.

Figure 4(a) shows the profiles of u_{DP} and u_{RP} , while Fig. 4(b) those of Q_{DT} and Q_{RT} . Again the profiles are different; nevertheless, Fig. 5 shows that the gross quantities M_{DP} and $\int_0^t M_{RP} dt$ as well as H_{DT} and $\int_0^t H_{RT} dt$ agree at any time t for any k , as the identities (3b) and (3c) predict. The relative errors of the numerical data are at the same level as before.

The identities in Eq. (3) deduced from the general theory in Ref. 10 have thus been demonstrated numerically.

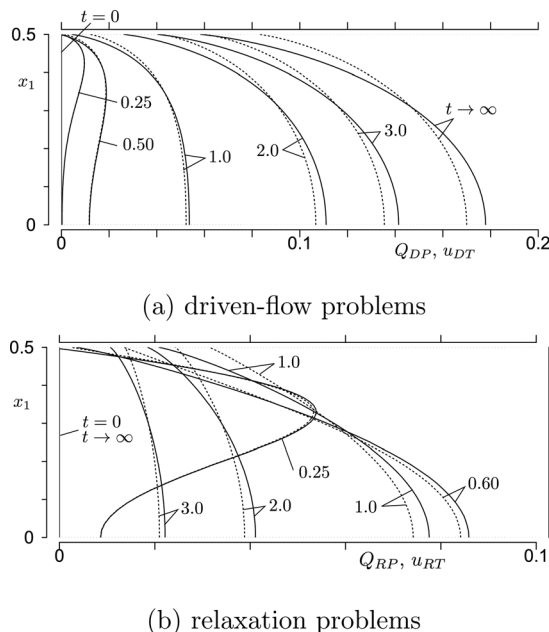
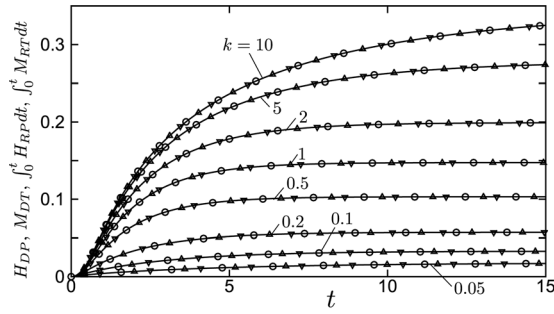
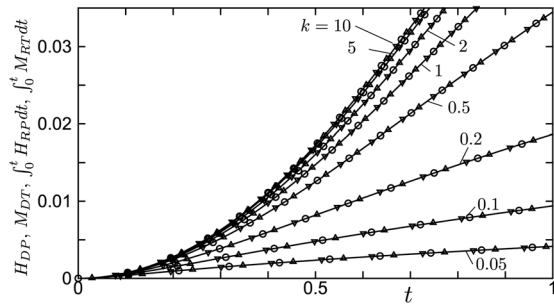


FIG. 2. Comparisons of mass and heat flow profiles in the half channel $0 \leq x_1 \leq 0.5$ at several values of t in the case of $k = 1$. I. (a) Q_{DP} and u_{DT} , (b) Q_{RP} and u_{RT} . Solid lines indicate Q_{DP} in (a) and Q_{RP} in (b), while dashed lines indicate u_{DT} in (a) and u_{RT} in (b).



(a) long time evolution

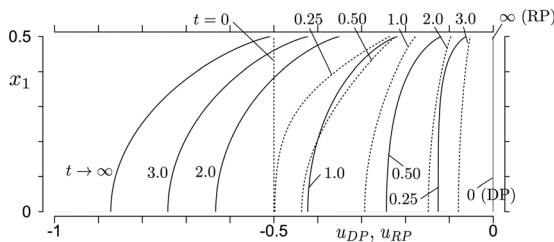


(b) short time evolution

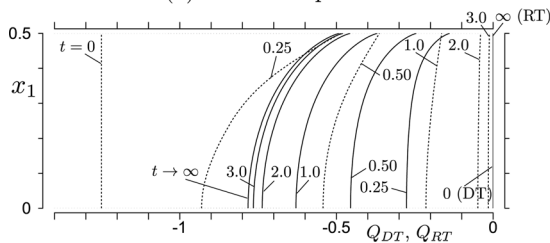
FIG. 3. Time evolution of the fluxes in Eq. (3a) for various k . (a) Long time evolution ($0 \leq t \leq 15$), (b) short time evolution ($0 \leq t \leq 1$). Solid lines indicate H_{DP} , open circles M_{DT} , open triangles $\int_0^t H_{RP} dt$, and open inverted triangles $\int_0^t M_{RT} dt$.

B. Velocity distribution function

As an example of the marginal VDF, we show F_{RP} of the relaxation problem (RP) in Fig. 6(a) and F_{DP} of the driven flow problem (DP) in Fig. 6(b) at various time t at position $x_1 = 0.397$ in the case of $k = 1$. As observed in Fig. 6(a), the former has two discontinuities for every fixed t and x_1 .

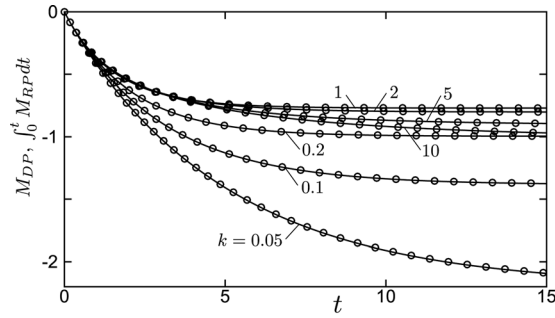


(a) mass flow profiles

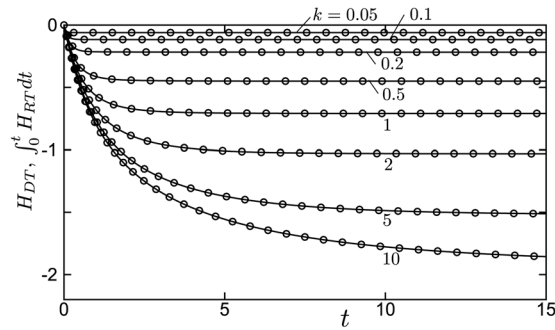


(b) heat flow profiles

FIG. 4. Comparisons of mass and heat flow profiles in the half channel $0 \leq x_1 \leq 0.5$ at several values of t in the case of $k = 1$. II. (a) u_{DP} and u_{RP} , (b) Q_{DT} and Q_{RT} . Solid lines indicate u_{DP} in (a) and Q_{DT} in (b), while dashed lines indicate u_{RP} in (a) and Q_{RT} in (b).



(a)



(b)

FIG. 5. Time evolution of the fluxes in Eqs. (3b) and (3c) for various k . (a) M_{DP} and $\int_0^t M_{RP} dt$, (b) H_{DT} and $\int_0^t H_{RT} dt$. Solid lines indicate M_{DP} in (a) and H_{DT} in (b), while open circles indicate $\int_0^t M_{RP} dt$ in (a) and $\int_0^t H_{RT} dt$ in (b).

They originate from the initial discontinuity on the plates caused by the difference between the boundary and initial data [compare Eqs. (1b) and (1f)] and propagate along the characteristics with decaying in time by intermolecular collisions. Detailed descriptions of the VDF discontinuity can be found in Refs. 16 and 17. The location of the discontinuities is easily identified as $x_1 = \pm 1/2 + \zeta_1 t$ ($\zeta_1 \leq 0$), and thus they are captured by the hybrid finite-difference scheme.¹⁵ On the other hand, in the driven-flow problem (DP), there is no difference between the boundary and initial data [compare Eqs. (1b) and (1d)], and accordingly F_{DP} is continuous [see Fig. 6(b)]. A close observation shows, however, that F_{DP} is not smooth at the same location as the discontinuity of F_{RP} , i.e., at $x_1 = \pm 1/2 + \zeta_1 t$ ($\zeta_1 \leq 0$), which is captured also by the use of the hybrid finite-difference scheme. The features described in this paragraph are shared with F_{DT} and F_{RT} .

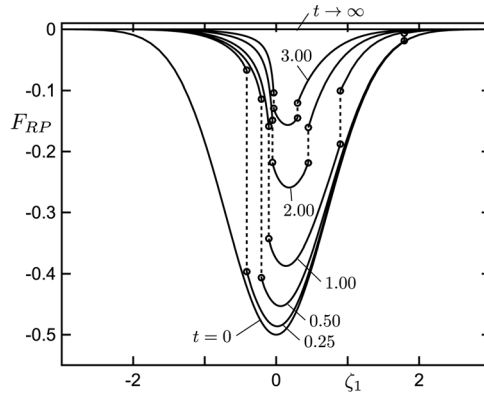
The reason of the derivative discontinuity seems less clear than that of the VDF discontinuity. However, we have a clear view, once we notice a relation between the relaxation problem [(RP) or (RT)] and the corresponding driven-flow problem [(DP) or (DT)]. Consider Eq. (1) for relaxation problem, i.e., $\alpha = RP$ or RT . Integrating it in time from 0 to t , we obtain an initial- and boundary-value problem for $\Phi_\alpha(t, x_1, \zeta) = \int_0^t \phi_\alpha(s, x_1, \zeta) ds$. The resulting problem for Φ_{RP} (or Φ_{RT}) is found to be identical to the problem for ϕ_{DP} (or ϕ_{DT}). In other words, it holds that

$$\phi_{DP}(t, x_1, \zeta) = \int_0^t \phi_{RP}(s, x_1, \zeta) ds, \quad (4a)$$

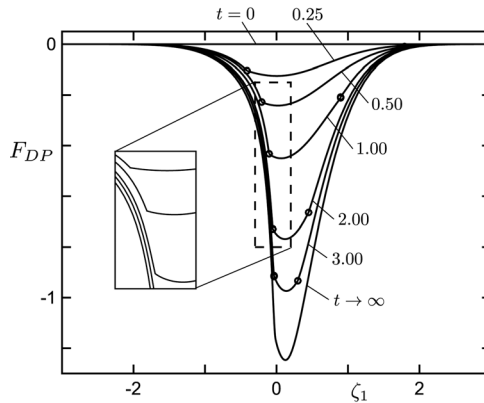
$$\phi_{DT}(t, x_1, \zeta) = \int_0^t \phi_{RT}(s, x_1, \zeta) ds. \quad (4b)$$

If we take time derivatives of ϕ_{DP} and ϕ_{DT} , they are discontinuous at the position where ϕ_{RP} and ϕ_{RT} are discontinuous. The derivative discontinuity in ζ_1 of the former two then follows directly.

It is obvious that the identities (3b) and (3c) follow directly from the above relation (4). The latter, however, implies a stronger statement that



(a) relaxation problem (RP)



(b) driven-flow problem (DP)

FIG. 6. Marginal velocity distribution functions F_{RP} and F_{DP} at several values of t at position $x_1 = 0.397$ in the case of $k = 1$. (a) F_{RP} , (b) F_{DP} . In both (a) and (b), open circles indicate the location of the discontinuities of F_{RP} and of the derivative discontinuities of F_{DP} with respect to ζ_1 . In (a), dashed lines indicate the discontinuities of F_{RP} .

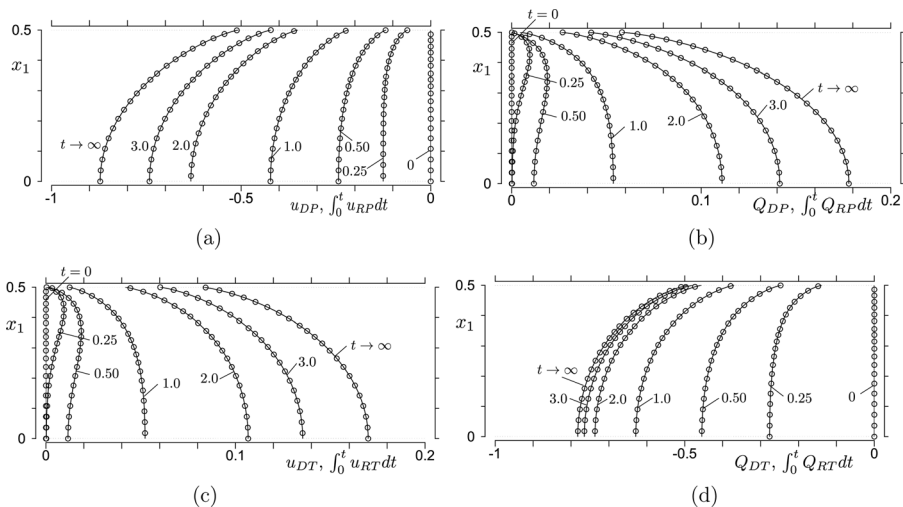


FIG. 7. Comparisons of the profiles of the fluxes in Eq. (5) in the case of $k = 1$. (a) u_{DP} and $\int_0^t u_{RP} dt$, (b) Q_{DP} and $\int_0^t Q_{RP} dt$, (c) u_{DT} and $\int_0^t u_{RT} dt$, and (d) Q_{DT} and $\int_0^t Q_{RT} dt$. Solid lines indicate u_{DP} in (a), Q_{DP} in (b), u_{DT} in (c), and Q_{DT} in (d); while open circles $\int_0^t u_{RP} dt$ in (a), $\int_0^t Q_{RP} dt$ in (b), $\int_0^t u_{RT} dt$ in (c), and $\int_0^t Q_{RT} dt$ in (d).

TABLE I. List of the demonstrated identities.

DP	RP	DT	RT	Equation	Figure
H_{DP}	$\int_0^t H_{RP} dt$	M_{DT}	$\int_0^t M_{RT} dt$	Eq. (3a)	Fig. 3
M_{DP}	$\int_0^t M_{RP} dt$	—	—	Eq. (3b)	Fig. 5(a)
—	—	H_{DT}	$\int_0^t H_{RT} dt$	Eq. (3c)	Fig. 5(b)
ϕ_{DP}	$\int_0^t \phi_{RP} dt$	—	—	Eq. (4a)	—
—	—	ϕ_{DT}	$\int_0^t \phi_{RT} dt$	Eq. (4b)	—
u_{DP}	$\int_0^t u_{RP} dt$	—	—	Eq. (5a)	Fig. 7(a)
Q_{DP}	$\int_0^t Q_{RP} dt$	—	—	Eq. (5a)	Fig. 7(b)
—	—	u_{DT}	$\int_0^t u_{RT} dt$	Eq. (5b)	Fig. 7(c)
—	—	Q_{DT}	$\int_0^t Q_{RT} dt$	Eq. (5b)	Fig. 7(d)

$$u_{DP} = \int_0^t u_{RP} dt, \quad Q_{DP} = \int_0^t Q_{RP} dt, \quad (5a)$$

$$u_{DT} = \int_0^t u_{RT} dt, \quad Q_{DT} = \int_0^t Q_{RT} dt. \quad (5b)$$

In other words, the identities should hold at the profile level. Figure 7 shows comparisons between u_{DP} and $\int_0^t u_{RP} dt$ in (a), between Q_{DP} and $\int_0^t Q_{RP} dt$ in (b), between u_{DT} and $\int_0^t u_{RT} dt$ in (c), and between Q_{DT} and $\int_0^t Q_{RT} dt$ in (d) at various time t in the case of $k = 1$. The identities in Eq. (5) are demonstrated perfectly in the figure.

V. CONCLUSION

We have investigated four elemental flows of a rarefied gas in a channel, mainly in order to provide an illustrative example of the time-dependent reciprocity developed in Ref. 10. The numerical computations have been carried out by the use of the linearized BGK model with the diffuse reflection boundary condition. The results demonstrate that, as predicted, the reciprocal relations (3a)–(3c) hold for a wide range of the Knudsen number at any instant. The numerical solution also demonstrates a propagation of discontinuities of the VDF and its derivative into the gas region. The derivative discontinuities are observed even in the driven-flow problems, in which the initial and boundary data are continuously connected at the initial time on the boundary. This occurrence has been clarified in terms of a further detailed relation of the driven-flow problem to the corresponding relaxation problem, in which the VDF itself has discontinuities. The detailed relation further implies the identities between the mass- and heat-flow profiles in driven-flow problems and the time integrations of those in relaxation problems. This equivalence has also been demonstrated.

We conclude the paper with summarizing thus demonstrated identities in Table I.

ACKNOWLEDGMENTS

The present work is partially supported by KAKENHI from MEXT (Nos. 23360083 and 23246034).

¹S. K. Loyalka, “Kinetic theory of thermal transpiration and mechanocaloric effect. I,” *J. Chem. Phys.* **55**, 4497 (1971).

²L. Waldmann and H. Vestner, “On the theory of boundary conditions,” *Physica A* **80**, 523 (1975).

³H. Lang, “Second-order slip effects in Poiseuille flow,” *Phys. Fluids* **19**, 366 (1976).

⁴B. I. M. ten Bosch, J. J. M. Beenakker, and I. Kuščer, “Onsager symmetries in field-dependent flows of rarefied molecular gases,” *Physica A* **123**, 443 (1984).

⁵F. R. W. McCourt, J. J. M. Beenakker, W. E. Köhler, and I. Kuščer, *Nonequilibrium Phenomena in Polyatomic Gases* (Clarendon, Oxford, 1991), Vol. 2.

⁶V. I. Roldughin, “On the theory of thermal polarization of bodies in a rarefied gas flow,” *J. Non-Equilib. Thermodyn.* **19**, 349 (1994).

⁷V. M. Zhdanov and V. I. Roldughin, “Non-equilibrium thermodynamics and kinetic theory of rarefied gases,” *Phys. Usp.* **41**, 349 (1998).

⁸S. Takata, “Symmetry of the linearized Boltzmann equation and its application,” *J. Stat. Phys.* **136**, 751 (2009).

- ⁹S. Takata, "Symmetry of the linearized Boltzmann equation II. Entropy production and Onsager–Casimir relation," *J. Stat. Phys.* **136**, 945 (2009).
- ¹⁰S. Takata, "Symmetry of the unsteady linearized Boltzmann equation in a fixed bounded domain," *J. Stat. Phys.* **140**, 985 (2010).
- ¹¹R. Kubo, M. Toda, and N. Hashitsume, *Statistical Physics II, Nonequilibrium Statistical Mechanics*, 2nd edn. (Springer, Berlin, 1991), Chap. 4.
- ¹²N. Pottier, *Nonequilibrium Statistical Physics* (Oxford University Press, New York, 2010).
- ¹³P. L. Bhatnagar, E. P. Gross, and M. Krook, "A model for collision processes in gases. I. Small amplitude processes in charged and neutral one-component systems," *Phys. Rev.* **94**, 511 (1954).
- ¹⁴P. Welander, "On the temperature jump in a rarefied gas," *Ark. Fys.* **7**, 507 (1954).
- ¹⁵Y. Sone and H. Sugimoto, "Strong evaporation from a plane condensed phase," in *Adiabatic Waves in Liquid-Vapor Systems*, edited by G. E. A. Meier and P. A. Thompson (Springer, Berlin, 1990), p. 293.
- ¹⁶Y. Sone and S. Takata, "Discontinuity of the velocity distribution function in a rarefied gas around a convex body and the S layer at the bottom of the Knudsen layer," *Transp. Theory Stat. Phys.* **21**, 501 (1992).
- ¹⁷Y. Sone, *Molecular Gas Dynamics* (Birkhäuser, Boston, 2007) (as of Dec. 2011, suppl. notes and errata are available at <http://hdl.handle.net/2433/66098>).
- ¹⁸The initial data of (DT) and (RT) for ψ do not satisfy the linearized Boltzmann equation (LBE). However, if we consider a solution of LBE realizing the temperature distribution $T_0(1 + C_{DT}x_1)$, the initial data of (DT) is the part which is responsible for the linear growth of temperature in x_1 , while the initial data of (RT) is the part which is responsible for the associated uniform heat flow. Splitting initial data in this way makes sense because of the linearized framework.
- ¹⁹K. Aoki, Y. Sone, K. Nishino, and H. Sugimoto, "Numerical analysis of unsteady motion of a rarefied gas caused by sudden changes of wall temperature with special interest in the propagation of a discontinuity in the velocity distribution function," in *Rarefied Gas Dynamics*, edited by A. E. Beylich (VCH, Weinheim, 1991), p. 222.